Electrochemistry

Deutsche Ausgabe: DOI: 10.1002/ange.201506963
Internationale Ausgabe: DOI: 10.1002/anie.201506963

Single-Nanoparticle Collision Events: Tunneling Electron Transfer on a Titanium Dioxide Passivated n-Silicon Electrode

*Hyun S. Ahn and Allen J. Bard**

Abstract: *Single-nanoparticle collisions were observed on an n-type silicon electrode (600 μm diameter) passivated by a thin layer of amorphous TiO_2, where the current steps occurred by tunneling electron transfer. The observed collision frequency was in reasonable agreement with that predicted from theory. The isolated electrode, after a collision experiment, with a Pt/TiO_2/n-Si architecture was shown to retain the photoelectrochemical properties of n-Si without photocorrosion or current decay. The Pt/TiO_2/n-Si electrode produced 19 mA cm^{-2} of photocurrent density under 100 mW cm^{-2} irradiation from a xenon lamp during oxygen evolution without current fading for over 12 h.*

Stochastic single-nanoparticle (NP) collision events on an electrode have been recently investigated by using amperometry[1–4] to provide important insights into the properties of individual NPs (i.e., size and catalytic activity) that are not easily accessible through conventional ensemble measurements. Current-amplification techniques, such as hydrazine oxidation catalysis on Pt NPs, were typically used to observe small currents (in the order of pA) associated with single-particle collision events.[4] The amplification is made possible by the superior electrocatalytic ability for hydrazine oxidation of Pt compared to the measuring gold ultramicroelectrode (UME). Recently, a more sensitive method for the observation of single-NP collisions was developed, where we showed that the electrodeposition of a thin amorphous TiO_2 layer can passivate a UME surface, thereby minimizing the background current.[5] Single-NP collision events have been observed by tunneling electron transfer to the NP, which was turned on by metal NP collision on an ultrathin (on the order of nanometers) TiO_2 layer. A single NP was isolated by this method, monitored by amperometry, and its size confirmed by using electron microscopy. Although this method of single-NP collision monitoring on a passivated UME is appealing, it also demands implementation of an already small ($d < 1$ μm) UME in order to achieve pinhole-free passivation.[5] In addition, only a limited number of stochastic NP collision events were observed because of the small size of the electrode compared to that of the NP ($d_{UME}/d_{NP} = 5$).[5] Herein we extend the concept of monitoring NP collision by tunneling electron transfer to larger electrodes. Tunneling NP collision experiments and the statistical analysis of the data were performed for the first time on a large electrode (n-type Si {100}, 0.001–0.005 Ω cm, 600 μm diameter). Despite the large size of the electrode, the background current was suppressed upon TiO_2 passivation (Figures 1 and 2). Owing to the large electrode size, a sufficient number of NP collision events could be monitored, allowing for collision frequency analysis. Furthermore, the tunneling electrode generated by an NP landing on an n-Si surface permitted the prolonged use of the underlying silicon as a semiconductor photoelectrode, because photocorrosion of the n-Si was effectively prevented by physical blockage of oxygen and water diffusion to the silicon surface.

The n-Si (100) electrodes used in the NP collision experiments were defined by use of masking tape. Typically, a 2 × 2 cm piece of n-Si was washed with HF to remove the native oxide layer, and then cleaned with deionized water. Electrically insulating masking tape with a 600 μm diameter hole was used to define the electrode (see the Supporting Information for details). Electrodeposition of amorphous TiO_2 was performed in an aqueous bath of $TiCl_3$ (15 mM, pH 2.3, Figure 2) as described previously,[6,7] and the deposition progress was monitored by photooxidation of 1,1′-ferrocenedimethanol (FcDM). As shown in Figure 3, approximately 15% of the photooxidation current remained after TiO_2 deposition, thus suggesting that the n-Si surface coverage was 85%. TiO_2 deposition was stopped at 80–86% coverage for all electrodes, in order to ensure a thin tunneling layer (ca. 1 nm thickness as estimated by atomic force microscopy and optical profilometry; see the Supporting Information and Figure S2 and S3). The TiO_2-deposited electrode was then thoroughly dried at room temperature to ensure full dehydration of the deposited film. The pinholes and uncovered n-Si area were then self-passivated by growth of an SiO_2 layer formed by immersing the electrode in oxygen-saturated water for 72 h. Previous studies indicate that under these conditions, an SiO_2 layer of thickness greater than 2 nm would grow,[8] and thus effectively block tunneling electron transfer.[9] Accordingly, no NP collision events were observed with an SiO_2-passivated electrode in the absence of TiO_2 treatment (Figure S4).

An electrode that was prepared for NP collision experiments, after TiO_2 deposition and SiO_2 self-passivation of pinholes, showed no current for photooxidation of 1 mM FcDM (Figure 3). Because n-type semiconductors do not ordinarily drive oxidation reactions in the dark, a reduction reaction was chosen for the observation of NP collision events. Detection of NP collisions was carried out by monitoring current transients by chronoamperometry in a solution containing 6 mM potassium ferricyanide and

[*] Dr. H. S. Ahn, Prof. A. J. Bard
Center for Electrochemistry, Department of Chemistry
The University of Texas at Austin
Austin, TX 78712 (USA)
E-mail: ajbard@mail.utexas.edu

Supporting information for this article is available on the WWW under http://dx.doi.org/10.1002/anie.201506963.

 © 2015 Wiley-VCH Verlag GmbH & Co. KGaA, Weinheim

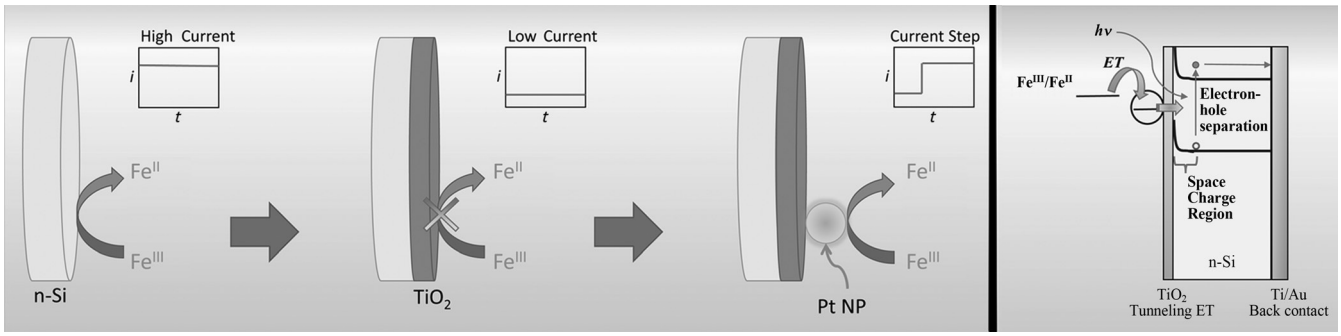

Figure 1. Electrode architecture showing amorphous TiO_2 layer that blocks the surface from processes that occur in solution. The dark current step associated with NP collision and turn-on of tunneling electron transfer is shown (left panel). A band structure diagram showing a series of electron-transfer steps in a typical PEC experiment of the Pt/TiO_2/n-Si electrode is shown on the right. A tunneling barrier to charge transfer exists in the TiO_2 layer.

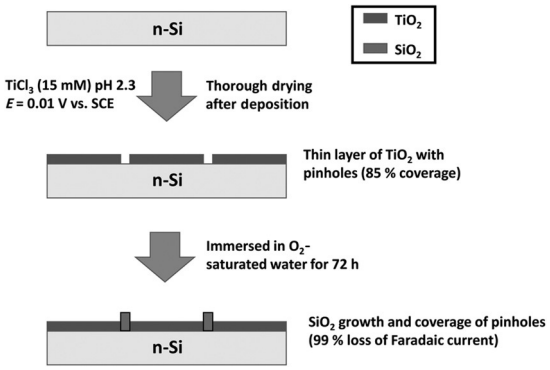

Figure 2. Fabrication of the TiO_2-passivated n-Si electrodes.

50 mM potassium phosphate buffer (pH 9). In the absence of Pt NPs, only a small background current was observed with a noise level of around 300 fA (Figure S5) and negligible change in the current level occurred. Suppression of the background current by the amorphous TiO_2 layer enabled the observation of NP collision events on a large (>100 μm) electrode for the first time. Upon introduction of Pt NPs (0.5, 1, 2, and 5 pM concentration, with the diameter of the Pt NP $d_{NP} \approx 50$ nm; see Figure 3 and 4), a steplike increase in the current was observed, arising from increased electrode area for ferricyanide reduction as each NP landed on the TiO_2 surface. This collision and sticking on the insulating surface introduces a large density of states compared to that of the analyte diffusing in solution (6 mM ferricyanide), and thus switches on the tunneling electron transfer. Similar phenomena have been theoretically predicted and experimentally observed.[9–11] Adhesion of the Pt NPs on the TiO_2 surface is believed to be strong, as evidenced by a clear steplike current response during amperometry (Figure 3), with little evidence of NPs leaving the surface. As a large number of NPs accumulate on the TiO_2 surface, the steplike responses become less defined (Figure S6), because the average background current increases. According to Equation (1),[12] each detected current step associated with the NP collision events were in the range 5–70 pA, which is in good agreement with the calculated steady-state current (76 pA for 50 nm NP) for a spherical UME.

$$i_{lim} = 4\pi nFDCr \ln 2 \quad (1)$$

In Equation (1), n is the number of electrons transferred (1 for ferricyanide), F is the Faraday constant, D is the diffusion coefficient of ferricyanide (6×10^{-6} cm^{2}s^{-1}), C is the analyte concentration (6 mM), and r is the radius of the electrode (25 nm). The difference in the histogram of collision events (centered at a calculated diameter of ca. 25 nm, Figure 3 d) and that obtained from light-scattering NP tracking data (dotted line in Figure 3 d) is attributed to minor fouling of the NP surface or tunneling-electron-transfer kinetics.[9,11] A couple of current steps larger than that expected for a 50 nm NP are attributed to aggregates landing on the electrode.

In our previous report on tunneling NP collisions on an insulating TiO_2 surface,[5] collision frequency analysis was not possible because of the limited number of collision events arising from the small electrode size ($d_{UME} < 1$ μm and $d_{UME}/d_{NP} = 5$). Statistically meaningful frequency analysis was possible in this work because of the larger number of stochastic collision events owing to the larger electrode size. The observed frequency of NP collision events is plotted against NP concentration in Figure 4, and shows a typical linear correlation of current step frequency as a function of NP concentration.[4] To compare the observed collision frequencies to those derived from theory, the following calculations were performed. The diffusion coefficient of NPs was estimated by the Stokes–Einstein relationship [Eq. (2)] and the collision frequency, as reported previously, by Equation (3).[4]

$$D_{NP} = \frac{k_B T}{6\pi\eta r_{NP}} \quad (2)$$

$$f_{NP\,collision} = 4 D_{NP} C_{NP} r_e N_A \quad (3)$$

In Equations (2) and (3), k_B is the Boltzmann constant, η is the solvent viscosity (water at 25 °C), r_{NP} is the NP radius, r_e is the radius of the electrode, C_{NP} is the effective NP concentration in experimental solution (see Figure S7), and N_A denotes Avogadro's number. The calculated NP collision frequency at 1 pM concentration was 0.46 Hz, in good agreement with the observed 0.20 Hz, considering the usual

© 2015 Wiley-VCH Verlag GmbH & Co. KGaA, Weinheim

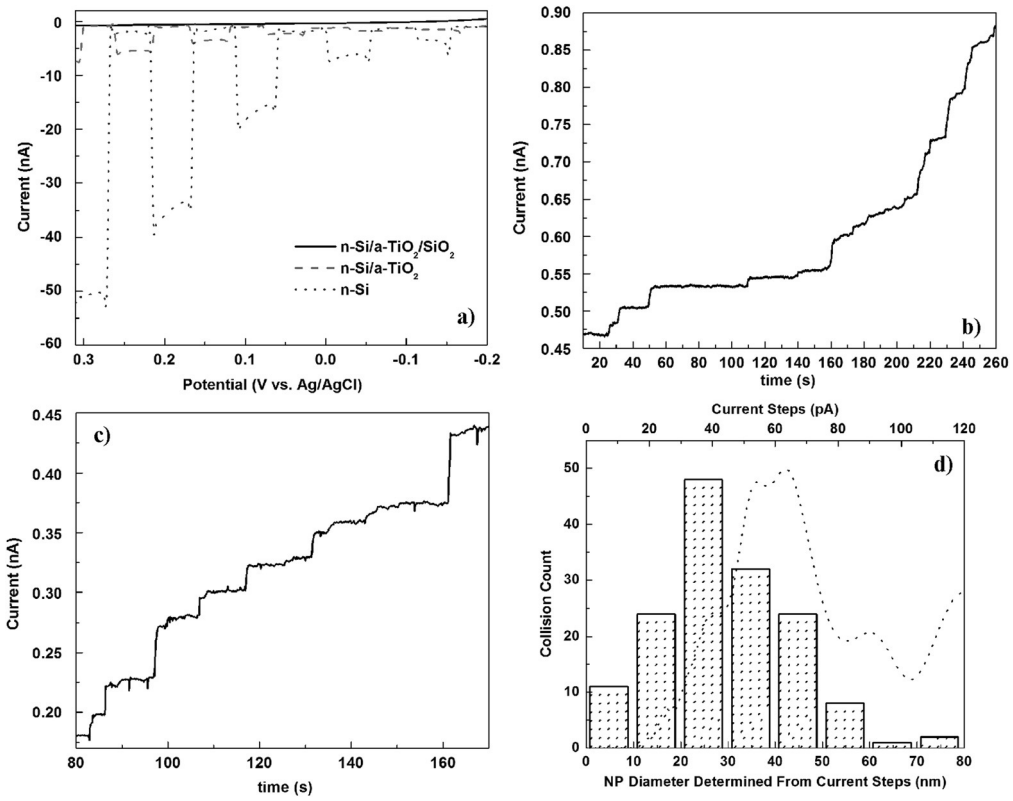

Figure 3. a) Chopped-light linear sweep voltammograms during photo-oxidation of 1 mM FcDM (50 mM phosphate pH 7, scan rate 10 $mV s^{-1}$, 100 $mW cm^{-2}$ xenon lamp): dotted trace was obtained from a freshly prepared n-type silicon (100), dashed trace was obtained after amorphous TiO_2 deposition, and solid line after SiO_2 passivation of pinholes. b, c) chronoamperograms of a TiO_2/n-Si electrode ($d = 600$ μm) in NP collision experiments in 0.5 pM NP concentration (analyte is 6 mM $K_3Fe(CN)_6$ in 50 mM phosphate buffer pH 9, −0.6 V, in absence of light). Clear current steps (5 to 70 pA) associated with NP landing and adsorption were observed. Background currents for (b) and (c) were 400 pA and 70 pA, respectively. d) Histogram of collision event step sizes. The dashed profile is the NP size distribution determined by a light-scattering NP tracking system.

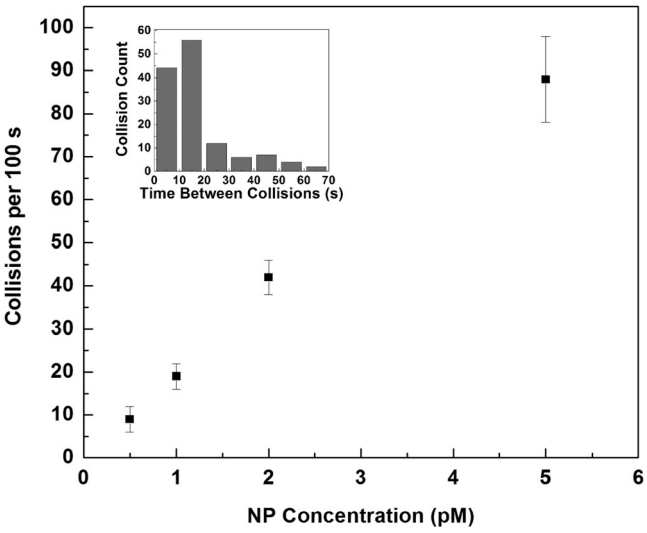

Figure 4. Number of observed current steps is plotted as a function of solution NP concentration. The good linear correlation suggests that the current steps indeed arise from NP collision events at the electrode. A histogram of time between each collisions is given in the inset.

uncertainty associated with measurements of stochastic events (Table S1).

The n-Si electrode was removed from the solution containing NPs after approximately 250 collision events in order to evaluate its photoelectrochemical properties. As shown in Figure 1, effective tunneling electron transfer should allow for an extended use of the photoelectrochemical properties of the underlying n-Si without experiencing photocorrosion. Chidsey,[13] Lewis,[14] and their respective co-workers have successfully demonstrated the formation of TiO_2 passivating layers on semiconductors by atomic layer deposition (ALD). The ALD TiO_2 film in the work by Chidsey and co-workers was annealed at 400 °C, and is probably rutile in phase.[13] Furthermore, the ALD films in the work by Lewis and co-workers were relatively thick films (ca. 143 nm) with current leakage.[14] Oxide films deposited by ALD tend to contain many pinholes unless they grow very thick (hundreds of nanometers);[15] in contrast, the electrodeposited TiO_2 film described here is amorphous and thin, which allows for tunneling electron transfer.[16] Our Pt-NP-decorated TiO_2/n-Si electrode was first subjected to a 1 mM solution of FcDM in 50 mM phosphate buffer (pH 7). In the chopped-light linear sweep voltammogram (LSV) shown in Figure 5a, a clear photoelectrochemical response similar to that of bare n-Si was observed (see Figure 1). Photoelectrochemical behavior of n-Si was also observed in the irreversible oxidation in sodium sulfite and the oxygen evolution reaction (OER, Figure 5b,c). Note that no photocurrent was observed on the electrode prior to Pt NP collisions (Figure 5). Interestingly, OER on the Pt/TiO_2/n-Si electrode continued for more than 12 h without any decrease of the photocurrent (Figure 5d), thus fulfilling the expectation that photoelectrochemical properties of silicon could be used for an extended period of time by physical blockage of oxygen and water and allowing only for tunneling electron transfer.

Some dark oxidation current (a function of potential) can be observed in Figure 5a–c in the absence of NPs. This is attributed to a small number of tunneling-electron-transfer events occurring through the space charge region (see

 © 2015 Wiley-VCH Verlag GmbH & Co. KGaA, Weinheim

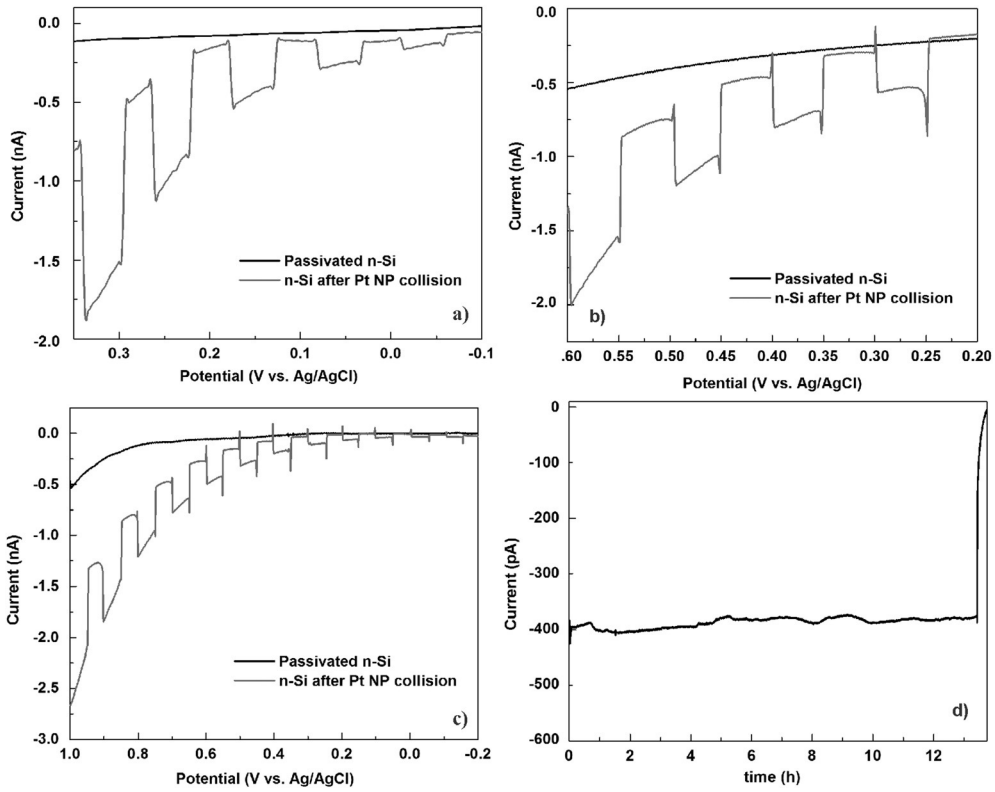

Figure 5. a) Chopped-light linear sweep voltammograms (LSVs) of TiO_2/n-Si electrode in the photooxidation of 1 mM FcDM (50 mM phosphate buffer pH 7, 100 $mW\,cm^{-2}$ xenon lamp). The TiO_2/n-Si electrode prior to Pt NP collision experiment (black trace) exhibited negligible current with no photoresponse. After NP collisions (ca. 1000 NPs, Pt/TiO_2/n-Si architecture, gray trace), however, clear evidence for the photooxidation of FcDM was observed, similar to that of freshly prepared n-Si. Scan rates for LSVs shown here are 10 $mV\,s^{-1}$. b) Chopped-light LSVs of TiO_2/n-Si (black) and Pt/TiO_2/n-Si (gray) for the photooxidation of 0.1 M Na_2SO_3. c) Chopped-light LSVs of TiO_2/n-Si (black) and Pt/TiO_2/n-Si (gray) for photoinduced OER at pH 7 (50 mM phosphate). d) Chronoamperogram of OER on Pt/TiO_2/n-Si (ca. 250 NPs of 50 nm radius, 1.2 V vs. Ag/AgCl) exhibiting 380 pA (19 $mA\,cm^{-2}$) without any decrease in current for over 12 h. The sharp break at 13.5 h is due to light shut off. Note that the difference in the current level for OER between (c) and (d) at similar potentials is due to some deactivation of NP surfaces and non-Faradaic charging of the large insulating electrode.

Figure 1). The tunneling current is a function of potential because the thickness and shape of the space charge region depends on the applied potential and the dopant density in the n-Si. The highly doped n-Si used in this work ($1\times10^{19}\,cm^{-3}$) may be the origin of the relatively large dark current because the high dopant concentration causes a decrease in thickness of the space charge region, thus rendering the tunneling barrier small. The increased dark current in the presence of NPs arises from the added channel for tunneling as the NPs adsorbed on TiO_2 supply a higher density of acceptor states for electron transfer. Also, in Figure 5d, the photocurrent does not immediately drop to zero upon extinction of light but rather exhibits a transient behavior. We attribute this phenomenon to a combination of some capacitive charging (including charge trapped states in the oxide) of the TiO_2/SiO_2 on the electrode under irradiation and some thermal relaxation of the solution temperature. Irradiation of the reaction cell (ca. 10 mL in volume) causes considerable increase in the solution temperature (42 °C after 10 h irradiation; the local temperature near the electrode is estimated to be higher).

The OER photocurrent density observed from the Pt/TiO_2/n-Si electrode was 0.13 $\mu A\,cm^{-2}$ when normalized by the whole electrode area (600 μm diameter disk, see the Supporting Information for detailed calculations). However, tunneling electron transfer is only allowed on TiO_2 sites that are in contact with the Pt NPs, therefore the surface area of the Pt NPs should define the area of the electrode participating in the photoelectrochemistry. The calculated photocurrent density normalized by the effective electrode area was 19 $mA\,cm^{-2}$ (250 NPs of 50 nm diameter, see the Supporting Information for detailed calculations), similar to that observed by Chidsey and co-workers.[13] The overlap of the diffusion layers of adjacent particles means that the actual photocurrent density may be lower, however, the value of 19 $mA\,cm^{-2}$ expressed here may serve as the upper limit.

In summary, we have demonstrated tunneling NP collision experiments on a large ($d = 600$ μm) semiconductor electrode. Initiation of the tunneling electron transfer was observed by the introduction of a large density of states at the surface of a thin insulating layer upon landing of a NP. Collision frequency analysis was achievable for tunneling collisions and were shown to agree with the theoretical projections. The tunneling NP electrode of the structure Pt/TiO_2/n-Si exhibited photoelectrochemical properties of the underlying n-Si by tunneling electron transfer, but was yet unmarred by photocorrosion that is characteristic of unprotected n-Si. Photoelectrochemical OER was observed on the prepared Pt/TiO_2/n-Si electrode for more than 12 h. We expect expanded applications of this surface passivation technique to other materials exhibiting photocorrosion behavior similar to silicon. Furthermore, the background current suppression by the passivation method presented in this contribution may be applied to other conducting and semiconducting electrodes for the enrichment of single-nano-object electrochemistry.

© 2015 Wiley-VCH Verlag GmbH & Co. KGaA, Weinheim

Acknowledgements

This work was supported by the NSF CCI Solar Fuels grant (CHE-1305124) and the National Science Foundation (grant no. CHE-1405248).

Keywords: electrochemistry · nanoparticles · photoelectrochemistry · surface passivation · tunneling

How to cite: *Angew. Chem. Int. Ed.* **2015**, *54*, 13753–13757
Angew. Chem. **2015**, *127*, 13957–13961

[1] X. Xiao, A. J. Bard, *J. Am. Chem. Soc.* **2007**, *129*, 9610.
[2] Y.-G. Zhou, N. V. Rees, J. Pillay, R. Tshikhudo, S. Vilakazi, R. G. Compton, *Chem. Commun.* **2012**, *48*, 224.
[3] S. E. F. Kleijn, S. C. S. Lai, T. S. Miller, A. I. Yanson, M. T. M. Koper, P. R. Unwin, *J. Am. Chem. Soc.* **2012**, *134*, 18558.
[4] S. J. Kwon, H. Zhou, F.-R. F. Fan, V. Vorobyev, B. Zhang, A. J. Bard, *Phys. Chem. Chem. Phys.* **2011**, *13*, 5394.
[5] J. Kim, B.-K. Kim, S. K. Cho, A. J. Bard, *J. Am. Chem. Soc.* **2014**, *136*, 8173.
[6] L. Kavan, B. O'Regan, A. Kay, M. Grätzel, *J. Electroanal. Chem.* **1993**, *346*, 291.
[7] L. Kavan, T. Stoto, M. J. Grätzel, *J. Phys. Chem.* **1993**, *97*, 9493.
[8] M. Morita, T. Ohmi, E. Hasegawa, M. Kawakami, M. Ohwada, *J. Appl. Phys.* **1990**, *68*, 1272.
[9] J. Chazalviel, P. Allongue, *J. Am. Chem. Soc.* **2011**, *133*, 762.
[10] S. Lhenry, J. Jalkh, Y. R. Leroux, J. Ruiz, R. Ciganda, D. Astruc, P. Hapiot, *J. Am. Chem. Soc.* **2014**, *136*, 17950.
[11] J. B. Shein, L. M. H. Lai, P. K. Eggers, M. N. Paddon-Row, J. J. Gooding, *Langmuir* **2009**, *25*, 11121.
[12] P. A. Bobbert, M. Wind, J. Vlieger, *J. Physica A* **1987**, *141*, 58.
[13] Y. W. Chen, J. D. Prange, S. Duhnen, Y. Park, M. Gunji, C. E. D. Chidsey, P. C. McIntyre, *Nat. Mater.* **2011**, *10*, 539.
[14] S. Hu, M. R. Shaner, J. A. Beardslee, M. Lichterman, B. S. Brunschwig, N. S. Lewis, *Science* **2014**, *344*, 1005.
[15] A. K. Satpati, N. Arroyo-Currás, L. Ji, E. T. Yu, A. J. Bard, *Chem. Mater.* **2013**, *25*, 4165.
[16] C. Renault, K. Marchuk, H. S. Ahn, E. J. Titus, J. Kim, K. A. Willets, A. J. Bard, *Anal. Chem.* **2015**, *87*, 5730.

Received: July 27, 2015
Published online: September 17, 2015

 © 2015 Wiley-VCH Verlag GmbH & Co. KGaA, Weinheim